Experimental and Theoretical Studies of the Electronic Spectra of Mixed Framework Phosphates of Zr and Co

Yulia V. Frolova,[†,‡] Vasilii I. Avdeev,[‡] Sergey Ph. Ruzankin,[‡] Georgii M. Zhidomirov,[‡] Martin A. Fedotov,[‡] and Vladislav A. Sadykov*[,†,‡]

Novosibirsk State University, and Boreskov Institute of Catalysis, Novosibirsk 630090, Russia

Received: August 8, 2003; In Final Form: March 25, 2004

Electronic diffuse reflectance spectra were acquired for samples of mixed framework phosphates of zirconium and cobalt calcined in a broad temperature range (40−900 °C). Analysis of the spectral features and their comparison with data available for different cobalt phosphates and CoAPO revealed that in complex framework phosphates the nearest coordination sphere of Co cations corresponds mainly to the oxygen polyhedra with a low coordination number such as the tetrahedron, pyramid, etc. In the frames of the time-dependent DFT method (TDDFT), the electronic excitation energies for cobalt cations in different oxygen environments have been calculated. The results obtained allowed us to describe the spectra of mixed cobalt−zirconium phosphates of various crystallinity both in the d−d transition and charge-transfer ranges with due regard for the simultaneous presence of Co cations in different coordination polyhedra and spin states. In prediction of the spectral features, the approach used in this work was shown to reasonably agree with the traditional concepts and experience in analysis of the electronic spectra of transition metal cations in their complexes and inorganic frameworks.

1. Introduction

Zeolites, complex phosphates, silicates, aluminates, etc., constitute a broad class of catalysts containing transition metal cations as active components. This includes cobalt aluminates and cobalt-containing zeolites as active catalysts of NO_x selective reduction by hydrocarbons in an excess of oxygen;[1,2] Co−ZSM-5 and Co−β-zeolites as active catalysts for the propane ammonolysis into acetonitrile,[3] etc. Recently, catalysts based on complex framework phosphates of Zr and Co or Mn were found to be very efficient in the oxidative dehydrogenation of propane into propylene at short contact times.[4,5] The active sites (AS) of these catalysts are comprised of the transition metal cations with properties determined by the oxygen environment belonging to the framework of zirconium phosphates. As a rule, AS includes only a limited number of atoms of the lattice surrounding a cation. The electronic structure of AS depends on the coordination number and the local geometry of the environment, which thus govern catalytic properties.

Cobalt-containing framework zirconium phosphates with the $NaZr_2(PO_4)_3$ (NZP) structure appear to be very attractive for systematic studies of those factors, since they possess a flexible lattice allowing realization of aliovalent (heterovalent) substitution both in cation and anion positions without its destruction.[6−9] Materials based upon those systems possess a high cationic (including protonic) conductivity, a high radiation and corrosion stability (attractive for such applications as radionuclides immobilization), as well as ultralow thermal expansion.[10−12] Aliovalent substitution allows us to tune into a broad range of the redox and acid−base properties of framework zirconium phosphates, which make them promising as catalysts for the processes of acid−base[13−15] and redox[16] types.

Earlier[17−22] genesis of the structure of complex framework zirconium phosphates including those containing Co cations was studied by using a combination of such methods as TEM, SAXS, EXAFS, XPD, ^{31}P and ^{27}Al MAS NMR, FTIRS, and UV−Vis DRS. The synthesis procedure includes a sol−gel route or a mechanical activation of the mixture of solid reagents—crystalline hydrates of inorganic salts—followed by aging of nanosized precursors in hydrothermal conditions and calcination. The nanosized precursors of framework phosphates—particles of sols—are comprised of the packages with the structure of layered zirconium phosphates, while stabilizing cations are bound with phosphate groups at the external surface of the Zr−O layers. In the course of subsequent hydrothermal treatment, stabilizing cations are incorporated between Zr cations, rearranging the structure of precursors into that of framework phosphates. Dependent upon the method of synthesis and the nature of a stabilizing cation, different types of the framework zirconium phosphate structures are known to be formed including cubic,[9] rhombohedral, and monoclinic[9,23,24] ones. For the cobalt-containing system, framework phosphates with a structure of the monoclinic or a cubic type stable to 800 °C under air were formed.[19] A detailed description of the genesis of the structure of complex Co-containing framework zirconium phosphates studied by using a combination of structural and spectral methods will be presented in a separate publication.[25]

The electronic spectra of those samples contained well-developed bands in the range of 15000−20000 cm^{-1} (d−d transitions) with a comparable intensity of the high-frequency and low-frequency components.[19] Following a traditional scheme used for cobalt-containing oxide systems,[26,27] these bands were assigned to Co^{2+} cations in the tetrahedral and octahedral coordination. Since extinction coefficients of Co^{2+} tetrahedral complexes are 1−2 orders of magnitude higher than those of the octahedral complexes,[28] Co cations appear to be mainly located in the octahedral positions of complex framework zirconium phosphates. However, for monoclinic framework

* Corresponding author. Tel: +7-3832-343763. Fax: +7-3832-343056. E-mail: sadykov@catalysis.nsk.su.
† Novosibirsk State University.
‡ Boreskov Institute of Catalysis.

10.1021/jp0363500 CCC: $27.50 © 2004 American Chemical Society
Published on Web 05/07/2004

phosphates, this assignment meets a lot of difficulty. While for the rhombohedral complex framework zirconium phosphates of NZP type, stabilizing cations such as Na, Li, etc., are indeed situated in a rather symmetric octahedral position usually denoted as M_1[6] (vide infra), these symmetric interstices are absent in the structure of monoclinic phases of such framework phosphates as $NiZr_4P_6O_{24}$,[29] $Li_2Zr_4P_6O_{24}$,[24] $Na_3Sc_2(PO_4)_3$,[30] and $Li_3Fe_2(PO_4)_3$.[23] Instead, as judged by the single-crystal X-ray diffraction data[29] and neutron diffraction results,[23,30] the nearest coordination sphere of those stabilizing cations is comprised of distorted tetrahedra, 5-fold polyhedra, etc. For dispersed Co-containing framework zirconium phosphates, X-ray results of Pet′kov et al.[31] are in favor of Co location in the tetrahedral positions as well.

These results necessitate a more detailed analysis of the electronic spectra assignment of complex framework cobalt−zirconium phosphates by using both experimental and theoretical approaches. The main problem to be considered here is whether a complex spectrum in the d−d transition range with bands up to 20000 cm^{-1} can be explained by the presence of Co cations having up to 4 oxygen anions in the first coordination sphere, while 1−2 anions are also present at distances exceeding the chemical bond length. If not, the presence of octahedral positions filled by Co in the structure of dispersed monoclinic cobalt−zirconium phosphates due to the cation positional disordering (a partial substitution of Zr by Co in the framework) is suggested. The first hypothesis is favored by the results of Sobalic et al.[32] on the electronic spectra assignment for Co cations located in a deformed six-membered ring of the ferrierite structure (β site). Using a combination of FTIRS, UV−Vis, and EXAFS data, these authors demonstrated that this site characterized by four bands at 16000, 17100, 18600, and 20600 cm^{-1} can be determined as a Co cation coordinated to four framework oxygen atoms at a distance of 1.99 Å, while two framework oxygen atoms are situated at a distance of 2.85 Å, exceeding the length of the chemical bond. What is also important is that the integral absorption coefficient for bands corresponding to this β site is equal to that for the Co cation in the α position (coordinated only by four oxygen atoms), which is characterized by a single band at 15000 cm^{-1}. Certainly, these conclusions would be more reliable if based upon theoretical analysis of the electronic spectra for a given coordination of Co cations.

On the other hand, for $Na_5Zr(PO_4)_3$ monoclinic phase, IRS data appear to be indicative of the statistical distribution of Na and Zr in ZrO_6 octahedra;[33] hence, the second hypothesis, namely, location of Co cations in the octahedral positions, could not be a priori excluded as well.

This paper presents diffuse reflectance spectra of complex framework Co−Zr phosphates prepared by a sol−gel route and calcined in a broad temperature range. X-ray diffraction and magnetic susceptibility measurements were used to follow effects of the phase composition and electronic state of Co cations on the features of these spectra. The spectral analysis has been carried out by comparing the experimental and theoretical spectra calculated in the frames of the density functional theory (DFT), taking into account the time-dependent perturbations.[34] This generalized DFT method realized in the work of Runge and Gross[35] was subsequently called the time-dependent density functional theory (TDDFT). Up to date, the TDDFT method was verified for calculation of the excitation energies, dynamic polarization, hyper-polarization, and Van der Waals dispersion coefficients for a broad range of relatively simple molecules.[36−39] Due to a number of factors beyond the scope of the present analysis, much less experience was accumulated in calculations of electronic properties for systems containing transition metals.[40−42] This work is one of the attempts to apply the TDDFT method for calculations of the electronic spectra of complexes containing transition metals in different spin states.

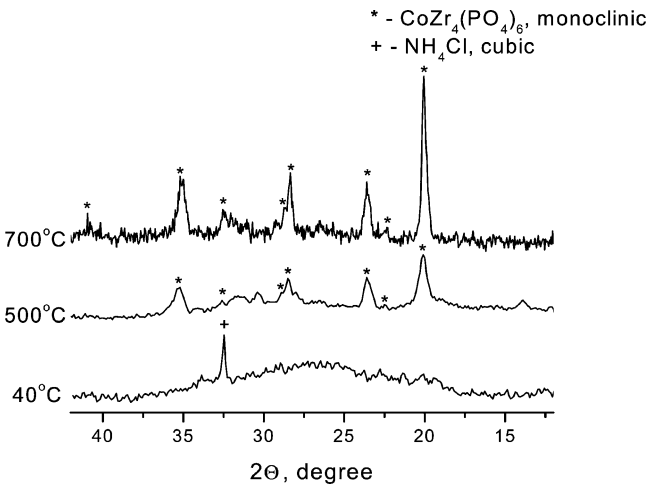

Figure 1. X-ray diffraction pattern for $CoZr_4(PO_4)_6$ samples after calcinations at 40, 500, and 700 °C.

2. Methodology

2.1. Experimental. To prepare samples of a $CoZr_4(PO_4)_6$ system by a sol−gel method, a required amount of ammonium dihydrophosphate was added dropwise with constant stirring to the mixed water solution of zirconium oxochloride and cobalt nitrate taken in a stoichiometric ratio. A sol thus obtained with pH ∼ 1 was dried at 20−120 °C and calcined under air at temperatures in the range of 300−900 °C. In the X-ray diffraction pattern (a URD-63 diffractometer, Cu Kα radiation) of a sample dried at 40 °C, a halo was observed, thus evidencing its amorphous nature. In addition, reflexes corresponding to a cubic phase of ammonium chloride were detected. After calcination at 500−700 °C, only the crystalline $CoZr_4(PO_4)_6$ phase of the monoclinic structure was detected. The increase of the calcination temperature up to 700 °C increases the sample crystallinity, which is reflected in the narrowing of the diffraction peaks, their shift, and intensity redistribution (Figure 1). All freshly prepared samples are of a deep blue color. Samples dried at 40−100 °C turn pink after prolonged (for months) standing under air at room temperature due to their hydration. In this paper only freshly prepared samples are studied and discussed.

The DRS spectra of freshly synthesized samples were recorded by using a UV 2501 PC spectrometer and $BaSO_4$ as a reference in the 4000−10000 cm^{-1} and 11250−55000 cm^{-1} wavenumber ranges. To normalize spectra, after subtraction of the baseline, the experimental data were transformed into the Kubelka-Munk function $F(R) = (1 - R)^2/(2R)$, where $R = 1 - T/T_0$.[43]

Spectra deconvolution has been carried out by using an original CALC Program. This routine is based upon a modified Newton-Rafson algorithm[44] with a due regard for a priori distribution of the individual component form (the Beies method).

Magnetic susceptibility measurements at room temperature have been carried out by the Faraday method on the home-built (Boreskov Institute of Catalysis) magnetic balance. After correction for the diamagnetic contribution, the magnetic moments of Co cations were estimated (Table 1). The small

TABLE 1: Magnetic Moments of Co Cations

composition	$T_{calcination}$, °C	$\mu_{\phi\phi}$, M_B at H[a] 8.3 T	14.1 T
$CoZr_4(PO_4)_6$	20	3.15	3.12
	80	2.70	2.71
	500	2.61	2.64
	700	4.99	5.35

[a] Magnetic field of the balance, Tesla.

difference between the magnetic moments measured in different magnetic fields (Table 1) assumes an insignificant part of the ferromagnetic phase in samples. As follows from these results, for samples calcined at 700 °C, all Co^{2+} cations are in the high-spin state with values of the magnetic moment typical for the majority of structures and complexes containing this cation.[28,45] However, for samples calcined at lower temperatures, the average magnetic moment corresponds to a mixture of the low-spin and high-spin states (roughly in a 1:1 ratio for a sample dried at 40 °C).

In general, several factors could be responsible for low values of the observed magnetic moment of cobalt cations.

First, a part of the Co^{2+} cations can be oxidized into a low-spin Co^{3+} state.[46] This option can be excluded since no bands corresponding to Co^{3+} cations (~23000−25000 cm^{-1})[47] are observed in the d−d range (vide infra).

Second, the antiferromagnetic exchange interaction between Co cations can result in a low magnetic moment, which is usually observed in cobalt oxides at low temperatures.[46] This interaction requires an ordered arrangement of Co cations in some extended planes, which is not favored in mixed framework phosphates where Co content is low.[31]

Third, low-spin states of Co cations were also recently revealed for single-crystal samples of cobalt borate phosphate $Co_3[BPO_7]$.[48] In this compound, there are three specific types of Co coordination polyhedra: a trigonal bipyramid, a square pyramid, and a distorted octahedron. This implies that the appearance of a low-spin state of Co^{2+} cations correlates with a low-coordinated less symmetric oxygen environment. Here, the concentration of cobalt is rather high, and Co-containing polyhedra are connected by a combination of edge- and corner-sharing. Even in this case, the superexchange antiferromagnetic interaction between neighboring cobalt atoms, i.e., Co(1)−O(3)−Co(2) units, was shown to be very weak, so this compound was paramagnetic at room temperature.

Fourth, a low magnetic moment can be due to a strong ligand field effect realized in the case of Co cations coordinated by some chelating ligands.[28] This implies that a part of the Co cations is coordinated by phosphate groups in a manner typical for the chelating ligands; namely, at least two oxygen atoms of each phosphate group are bound with a given Co cation. This possibility is excluded for Co cations occupying regular M_2 positions in monoclinic framework zirconium phosphates,[31] which agrees with their high-spin state for well-crystalline samples annealed at 700 °C. For an apparently less crystalline sample calcined at 500 °C, a Co cation can occupy less energetically favorable positions where it is coordinated by 2−3 oxygen anions belonging to the same phosphate group. Indeed, similar intermediate M'_3 positions (distorted tetrahedra) are known to be occupied even by more bulky Li cations in the course of their diffusion in the NASICON-type $Li_3Ti_2(PO_4)_3$ phase.[49] For amorphous precursors—sols dried up to 80 °C, at the external surface of zirconium phosphates layers comprised of Zr cations bound by three-dentate phosphate groups—there also exists a possibility for a Co cation to be bound with two

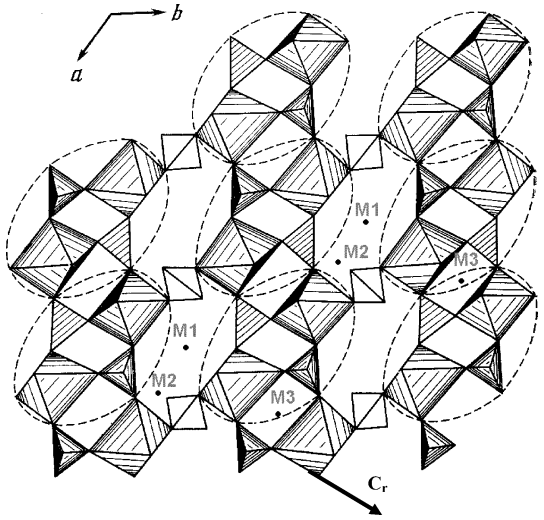

Figure 2. Framework arrangement in the $NaZr_2(PO_4)_3$ rhombohedral-type structure. $\mathbf{C_r}$ represents the axis of the rhombohedral structure, and *a* and *b* are axes of the monoclinic structure. M_1, M_2, and M_3 are positions of the guest (stabilizing) cations in the lattice by Alamo and Roy.[8]

neighboring phosphate groups (each bearing a 1− charge) in such a way that two or three oxygen atoms of each phosphate group can be involved in formation of a distorted tetrahedral or 5-fold coordination sphere. In sols dried and calcined at temperatures not exceeding 200−300 °C, ammonia and water molecules are retained in the lattice[19] and could also enter into the coordination sphere of a part of the Co cations along with the oxygen anions of phosphate groups, making chelating-type coordination less probable. Note that observed magnetic moment versus temperature of calcinations passed through a minimum reached for the sample calcined at 500 °C (Table 1), which appears to be reflected in the intensity of absorption in the UV range (vide infra). The driving force for rearranging of the Co cations coordination environment seems to be the sol dehydration and ammonium chloride decomposition (hence, progressive loss of water as well as ammonia molecules from the cations first coordination sphere) favoring stronger interaction between the cobalt cations and phosphate groups.

Hence, low-spin configurations of Co^{2+} cations in complex framework zirconium phosphates can appear due to the existence of low-symmetry coordination polyhedra (as in the $Co_3[BPO_7]$) and/or a strong ligand field effect.

2.2. Theoretical Models of the Co Cation Coordination Environment in the $CoZr_4(PO_4)_6$ System. Main features of the rhombohedral and monoclinic phases arrangement are shown in Figures 2 and 3, correspondingly. As follows from these figures, in these phases, the main structural (so-called lantern[23]) unit (encircled) is identical, and only the mutual orientation of those units differs.

In the structure of rhombohedral framework zirconium phosphates, stabilizing cations can be situated in several positions. The first site M_1 has a coordination number 6 (nearly perfect octahedron) and is situated in the chains of ZrO_6 octahedra along the $\mathbf{c_r}$ axes (Figure 2). The second position M_2 is comprised of complex polyhedra with coordination number 8÷14 placed between the ZrO_6 octahedral chains (Figure 2). The third position M_3 is surrounded by the oxygen atoms forming a slightly distorted trigonal prism, and it can be occupied only by small cations. In the general case, cobalt cations can be situated in the octahedral M_1 positions occupied in the rhombohedral NZP structure by sodium cations, as well as in M_2 positions between the octahedral chains.

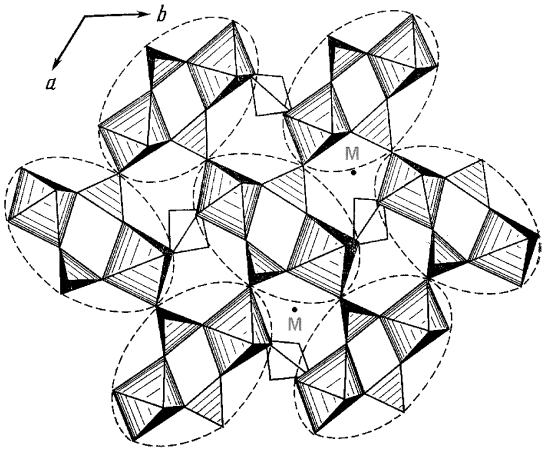

Figure 3. [001] view of the monoclinic structure of framework phosphates. M-position of a guest cation in the lattice by refs 9,29.

In the monoclinic structure of complex framework phosphates, due to rotation of the structural units, the regular M_1 octahedron and M_2 positions are merged into an irregular polyhedron M[9] (Figure 3). Stabilizing cations such as Li, Na,[30] Ni,[29] etc., were shown to be localized in such a polyhedron acquiring tetrahedral or 5-fold nearest coordination,[30] including distorted trigonal bipyramidal environment.[50]

To refine the structure of the dispersed binary framework phosphates of zirconium and 3d transition metals (Co, Mn, Ni, Cu, Zn), Pet'kov et al.[31] as reference data used the results of the X-ray full-profile refinement of the structure of a single-crystalline $NiZr_4(PO_4)_6$ sample. Similarity of the X-ray diffraction patterns for this sample and dispersed binary framework phosphates revealing their monoclinic symmetry was considered as an indication of their similar structural arrangement. In the first coordination sphere of a Ni cation, oxygen atoms form a strongly distorted tetrahedron with a mean Ni−O distance equal to 2.11 Å. The nearest oxygen atom from the second coordination sphere is situated at a distance of 2.833 Å. Since the ionic radii of Co and Ni cations are close to each other, a similar environment of cobalt cations in the crystalline $CoZr_4(PO_4)_6$ phase with a monoclinic symmetry shown in Figure 4 can be suggested. However, due to flexibility of the framework phosphate structure, pronounced relaxation of the structure is expected as dependent upon the degree of samples crystallinity. As a limiting case of the flexible structure, models of the relaxed coordination environment corresponding to the minimum of energy at a given electronic state of Co will be considered as well.

In the present work, as a first approximation, only oxygen environment of cobalt cations was taken into account when computing their electronic spectra. In all cases, the broken bands of the oxygen atoms with surrounding matrix were traditionally saturated with the hydrogen atoms. This approach is apparently not able to describe the appearance of low-spin states of Co cations, hence, their electronic state will be considered as a parameter. The aim of the present paper is thus restricted to elucidation of the effect of symmetry of the first and second coordination sphere of cobalt cations on the features of their electronic spectra. More detailed analysis of the electronic structure with a due regard for the effect of phosphate groups requires much more extended calculations and will be presented elsewhere. Using the data of the magnetic measurements, theoretical spectra have been calculated in order to explain the experimental data. Modeling was also applied to analyze the nature of the transition from the high-spin to the low-spin state.

2.3. Computational Details. For calculation of the geometry, total energy, and excitation energies, a hybrid exchange functional with Becke gradient corrections[51,52] was combined with the Lee−Yang−Parr correlation functional[53] (a B3LYP method). As an orbital basis, a 6-31G* set was used. The core electrons of cobalt were included into the effective CEP potential with the valence-split CEP-31G basis.[54,55] Calculations have been carried out by using a GAUSSIAN 98 software package.[56]

The general scheme of the electronic excitation energies and oscillator strength computation includes next steps. First of all, the full energy of chosen models of AS was computed for the high-spin ($2S + 1 = 4$) and low-spin ($2S + 1 = 2$) states. Two

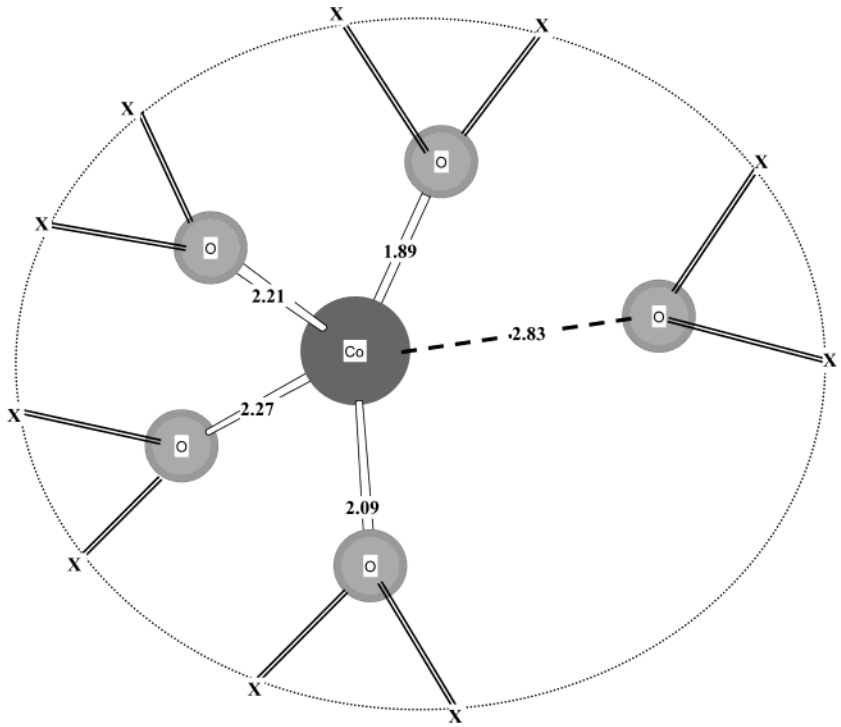

Figure 4. Arrangement of oxygen anions around Co cations in the rigid model of crystalline $CoZr_4(PO_4)_6$ phase following ref 29.

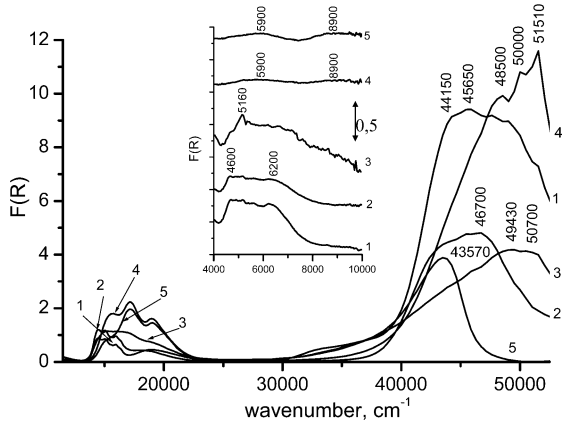

Figure 5. UV−Vis−NIR spectra of $CoZr_4(PO_4)_6$ samples after calcination at **1**: 40 °C, **2**: 300 °C, **3**: 500 °C, **4**: 700 °C, and **5**: 900 °C.

limiting cases were considered. For crystalline phases, the structure of the AS was first considered to be a rigid one. For amorphous samples, a labile structure of the oxygen framework was suggested, and full optimization of the AS geometry has been carried out. The next basic step consists of calculation of discrete spectra of the excited states by the TDDFT method including 20−25 energy transitions in the range of 3000−55000 cm^{-1} and corresponding oscillator strengths. From the point of view of the computing resources, this step is the most demanding. To compare with the experimental spectra, if required, the calculated discrete spectrum was broadened by applying the Lorentz distribution with a half width $\gamma \sim 2000$ cm^{-1}.

3. Experimental Spectra

Figure 5 presents the spectra of studied samples. The range of 4500−25000 cm^{-1} is due to d−d transitions, and the range of 35000−55000 cm^{-1} corresponds to the ligand−metal charge-transfer bands, i.e., from the $\sigma-\pi$ orbital of oxygen to a d-orbital of Co. Specially recorded spectra for the rhombohedral phase of ammonium zirconium phosphate calcined in the same temperature range (not shown for brevity) revealed that zirconium phosphate framework has no detectable absorption in the d−d range (>10000 cm^{-1}). In the UV range only very weak bands at ∼39000 and 45000 cm^{-1} with intensity less than 0.05 K-M units were observed, which is much less than the intensity of bands observed in this range for Co-containing samples (4−10 K-M units). This spectral specificity of Zr phosphate framework appears to be explained by its high covalency.[11,13] Bands at ∼4600, 5160, 5900, and 6200 cm^{-1} could be due not only to d−d transition in Co cations, but also to the overtones of the water molecules.[57]

Figure 6 shows deconvolution of the complex absorption bands for two samples of series considered here. For the sample dried at 40 °C, which is X-ray amorphous, a broad band at 4600−6200 cm^{-1} (Figure 5) and a triplet at 14400−16000 cm^{-1} along with a band at ∼19000 cm^{-1} are observed. After deconvolution, at least two groups of bands at ∼14400, 15150, 16000, and 16750 cm^{-1}, and at 18550, 20300, and 21600 cm^{-1} are revealed (Figure 6A). This implies that, in this sample, several types of Co cations in a somewhat different coordination environment are simultaneously present. In the UV range, at least 9 strong absorption bands can be selected (Figure 6), which also suggests the existence of several types of Co complexes. The absorption edge is located at ∼39700 cm^{-1}. Calcination at higher temperatures does not appreciably decrease the number of absorption components (and, hence, diversity of the types of

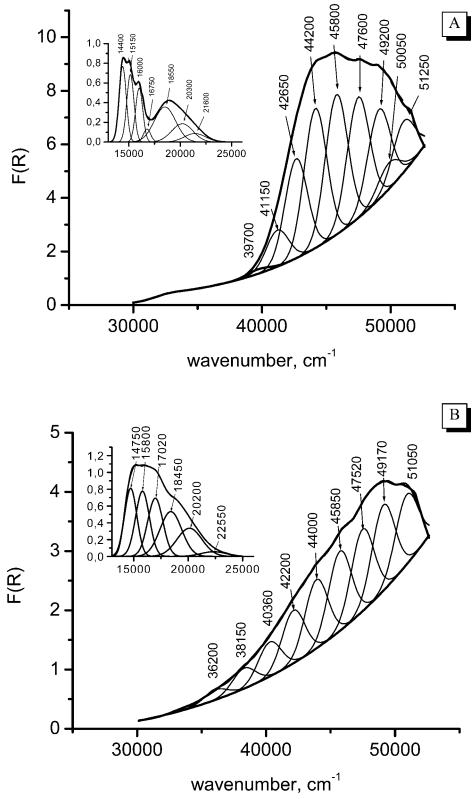

Figure 6. UV−Vis diffuse reflectance spectra of $CoZr_4(PO_4)_6$ samples after drying at 40 °C (A**)** or calcination at 500 °C (B**)**.

Co cations coordination), though causing some redistribution in their intensity and position.

Thus, calcination at 500 °C rearranges a sol structure into that of a crystalline (though apparently disordered) monoclinic phase of the mixed framework phosphate of Co and Zr (Figure 1). In the range of d−d transition, the spectral changes are small: some broadening and a blue shift of the bands (14750, 15800, 17020, 18450, 20200, and 22550 cm^{-1}) are observed (Figure 6B). Since absorption coefficients for cobalt cations in the tetrahedral and octahedral coordination differ by more than an order of magnitude,[28] a weak variation of the integral absorption in the visible region suggests that in this range of calcination temperatures the dominating type of the cobalt cations coordination is not changed appreciably. After calcination at 700 °C, the component at ∼17000 cm^{-1} becomes the most intense. Annealing at 900 °C decreases the intensity of a component at ∼15000 cm^{-1} while intensities of other bands in the d−d range remain unchanged.

On the other hand, spectral variation in the UV range is much more pronounced. The increase of the temperature of thermal treatment from 40 to 500 °C is accompanied by a decrease of the intensity of UV absorption and its high-frequency shift (Figure 5). For the sample calcined at 500 °C, a complex strongly asymmetric absorption is observed which is deconvoluted into nine individual absorption bands (Figure 6B). The absorption edge shifts to 36200 cm^{-1}, while the maximum of UV absorption moves to higher frequencies as compared with that for the amorphous sample (Figures 5 and 6). For the sample calcined at 700 °C, when the crystallization is completed, the intensity of UV bands increases again, while the absorption maximum position is preserved for this sample (Figure 5). After annealing at 900 °C, when the structure partially decomposes yielding Co pyrophosphate,[25] the intensity of absorption in the UV range declines again with a clearly expressed red shift. Due

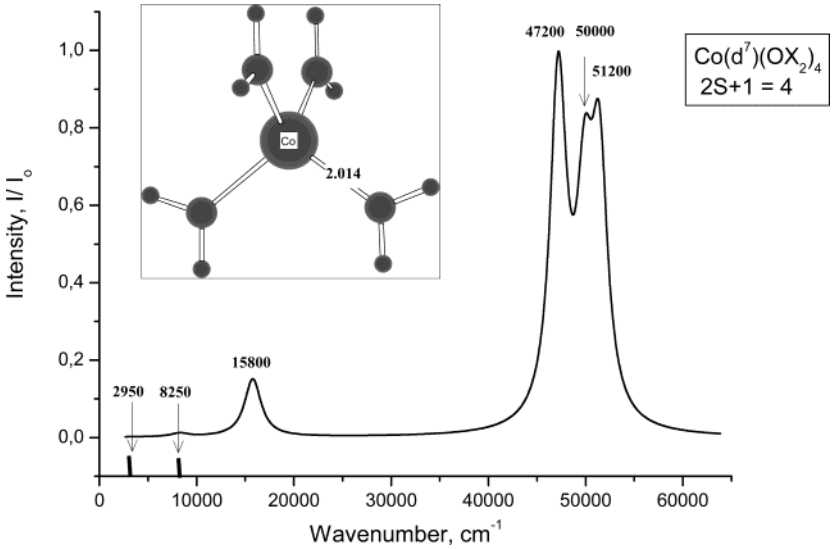

Figure 7. The calculated electronic spectrum for the high-spin state of the $[Co(d^7)(OX_2)_4]^{2+}$ complex with an optimized geometry.

to complexity of the phase composition, the spectral features for the latter sample will not be analyzed here.

The decline of the UV bands intensity with the temperature of calcinations followed by its increase after annealing at 700 °C clearly correlates with variation of the average magnetic moment of Co cations (Table 1) (vide infra).

The intensity of absorption in the d−d range (∼1 K-M units) for samples considered here (Co content 6 wt % or 0.72 mol/L) related per Co content was found to be comparable with that for CoAPO-5 and CoAPO-11 samples characterized in refs 57,58.

For those zeolite samples with a cobalt content ∼0.5 wt % (0.163 mol/L) calcined under air and then reduced by hydrogen at 623−673 K, similar positions of bands in the visible range (3−4 components in the ∼15000−20000 cm^{-1} range) with the maximum intensity ∼0.2 K-M units were observed. After such pretreatment, Co cations are predominantly in the tetrahedral coordination with a strong trigonal distortion (up to trigonal pyramidal environment) due to the presence of oxygen vacancies.[58] This assignment follows the pioneering UV−vis−NIR study of Klier on the CoA zeolite.[59] In the latter work, for ethylene−Co(II)A complexes similar positions and splitting of bands in the d−d spectral range were observed and theoretically treated as due to low-symmetry effects.

The intensity of DRS bands is well-known to also depend on the scattering ability of samples mainly determined by their particle size. For both types of systems—CoAPO and complex framework zirconium phosphates, the particle sizes are also comparable. Thus, the specific surface area of framework cobalt−zirconium phosphates varies in the range of ∼250 m^2/g (a sample dried at 40 °C, typical particle sizes in the range of 50−100 Å) to 40 m^2/g (a sample calcined at 900 °C, typical particle sizes in the range up to 300 Å). For CoAPO the specific surface area ∼200−300 m^2/g corresponds to mean particle sizes ∼50−100 Å.

For Co−Zr phosphates, the integral absorption in the d−d range estimated by the area under the absorption peaks (proportional to the oscillator strength[28]) is equal to 3575 cm^{-1} for the sample dried at 40 °C and 6241 cm^{-1} for the sample calcined at 500 °C. For CoAPO-5, the area under peaks in the same frequency range is ∼1720 cm^{-1}. A close value of the thus-estimated integral absorption for those two types of systems related to the cobalt concentration -(0.5−1.0) 10^3 L/(mol cm) suggests that in framework phosphates, Co cations are mainly in a low-coordinated environment as well. This coordination is close to the tetrahedral one or, at least, it is of a low-symmetry type ensuring a high value of the molar extinction coefficient, such as trigonal bipyramid, trigonal, tetragonal pyramid, etc.[28] Taking into account uncertainty in the scattering ability of particles and variation of the molar absorption coefficient within a factor of 2, this conclusion could be valid for at least half of the cobalt cations in complex framework phosphates. On the other hand, for these samples, the intensity of bands at ∼20000 cm^{-1} usually assigned to octahedrally coordinated Co cations[28] is comparable with the intensity of bands at ∼15000−18000 cm^{-1} corresponding to low-coordinated Co cations (Figure 5). Taking into account the usual ratio between absorption coefficients for tetrahedral and octahedral complexes (10^1−10^2),[28] this requires a much lower amount of low-coordinated Co cations. Hence, estimation of the relative amount of low-coordinated Co cations in our samples (vide supra) is certainly not in favor of relating high-frequency bands in the d−d range to octahedrally coordinated Co^{2+} cations.

4. Theoretical Analysis

4.1. Four-fold and Octahedrally Coordinated Complexes. Figure 7 shows a spectrum for the high-spin fully optimized $[Co(d^7)(OX_2)_4]^{2+}$ complex. The range of 2900−16000 cm^{-1} corresponds to d−d transitions, while the range at 45000−52000 cm^{-1} corresponds to the $\sigma,\pi(O) \rightarrow d(Co)$ charge-transfer bands. In the ideal tetrahedron classification, theoretical values of the transition energy at 2946, 8193, 8329, 15658, 15781, 15972 cm^{-1} and the region 40000−52000 cm^{-1} correspond to $^4A_2 \rightarrow {}^4T_2$, $^4A_2 \rightarrow {}^4T_1$, $^4A_2 \rightarrow {}^4T_1$ (P), and $\sigma,\pi(O) \rightarrow {}^4T_2$, $^4T_1$, $^4T_1$ (P) transitions, respectively. In our case, due to a weak perturbation of the cluster by the matrix X, the symmetry of the cluster decreases to D_2, and degenerate states become completely split. Table 2 presents complete classification of these transitions. Here, for comparison, the energies of the excited states for the low-spin state of cobalt (2+) are shown as well. Without taking into account specificity of the phosphate groups as chelating ligands, the high-spin ^4A state is the ground state, since the low-spin one has the energy higher by 33 kcal/mol.

For the low-spin state with distorted square planar coordination, oscillator strength corresponding to d−d transitions in the range >10000 cm^{-1} is much lower as compared with those for the high-spin state. While the oscillator strength for charge-

TABLE 2: Excitation-State Spectrum of the Labile Optimized Four-fold Coordinated Complex $[Co(d_7)(OX_2)_4]^{2+}$ with D_2 Symmetry of a Weakly Distorted Tetrahedron for the High-Spin State and C_1 Symmetry of a Weakly Distorted Square for the Low-Spin State

high−spin state (2S + 1 = 4)			low-spin state (2S + 1 = 2)	
symmetry, (group D_2)	transition energy, cm^{-1}	oscillator strength, $f \times 10^4$	transition energy, cm^{-1}	oscillator strength $f \times 10^4$
$^4B_2$	2946	0.00	2722	0.25
$^4B3$	8193	0.58	3473	0.13
$^4B_1$	8329	0.56	6613	0.37
$^4B_3$	15658	12.82	7166	0.21
$^4B_2$	15781	12.92	8292	0.02
$^4B_2$	15972	8.30	8484	0.00
^4A	45162	0.00	3615	0.02
$^4B_1$	47130	101.53	17654	0.06
$^4B_3$	47234	97.07	18321	0.03
$^4B_1$	47743	4.58	22831	0.04
$^4B_3$	47752	1.33	29065	0.03
$^4B_2$	49078	0.37	31829	71.85
^4A	49356	0.00	32583	110.84
$^4B_2$	49495	1.72	34969	8.27
^4A	49909	114.40	36615	0.07
^4A	50632	0.00	37300	0.03
^4A	50708	0.00	37483	2.20
$^4B_3$	51353	77.57	38314	2.87
$^4B_1$	51464	69.47	39284	56.49

transfer bands is comparable by magnitude for both high-spin and low-spin states, they strongly differ by their energy.

Comparison of the calculated spectra for the labile tetrahedral high-spin $[Co(d^7)(OX_2)_4]^{2+}$ complex (Figure 7, Table 2) and low-spin distorted square complex (Table 2) with the experimental spectrum (Figure 6) revealed that spectra of neither the amorphous sample dried at 40 °C nor the relatively crystalline sample calcined at 500 °C could be assigned exclusively to those complexes. The most apparent difference is that for both model complexes intense UV bands at 43000−45000 cm^{-1} are absent while being observed in the experimental spectra. In addition, the band at ∼8000 cm^{-1} predicted by calculations for a slightly distorted tetrahedron is absent in the spectrum of the amorphous sample. Nevertheless, it is worth mentioning that for the tetrahedral complexes of Co^{2+}, such as $CoCl_4^{2-}$, the bands at 4780, 5100, 14300, and 14900 cm^{-1} are observed,[28] which agree well both by the position and their splitting with the results of calculations. Similar good agreement was observed for the UV range as well. In the spectra of this complex, two intense bands at 42735 and 46085 cm^{-1} are observed with a less intense band at 45000 cm^{-1} situated between, which correspond to the electrical dipole-allowed $^4A_2-^4T_2$ transitions. For the oxygen environment, our calculations predict two intense bands at 47200 and 51200 cm^{-1} with the less intense band situated between them at 50000 cm^{-1} observed as a shoulder (Figure 7). Apparently, substitution of Cl for oxygen as a ligand in the coordination sphere of Co cations only somewhat shifts the absorption bands to higher frequencies.

For optimized high-spin octahedral complexes of Co^{2+} with slightly distorted C_{2h} symmetry (Table 3), as expected,[28] intensities of bands in the d−d range are much lower as compared with 4-fold coordinated complexes. To the contrary, positions of the most intense charge-transfer bands (∼48000 cm^{-1}) are close to those for tetrahedral complexes (cf. Tables 2 and 3), while their intensities are higher. Again, experimental spectra could not be assigned to those complexes due to the absence of experimentally observed intense bands in the 43000−45000 cm^{-1} range in their calculated spectrum, not considering very weak absorption in the d−d range.

TABLE 3: Excitation State Spectrum of Optimized Six-fold Coordinated Complex $[Co(OX_2)_6]^{2+}$ [a]

high−spin state (2S + 1 = 4) - ^4Bg		
symmetry	energy, cm^{-1}	oscillator strength, $f \times 10^4$
^4B_g	5570	0. 00
^4A_g	5745	0. 00
^4B_g	12090.1	0. 00
^4A_g	16818.9	0. 00
^4A_g	16946.3	0. 00
^4A_g	20976.7	0. 00
^4B_g	48009.7	0. 00
^4B_g	48023.4	190.44
^4B_u	48141.2	197.01
^4A_u	48179.1	76.92
^4B_u	50536.6	0. 00
^4B_g	51332.7	0. 00
^4A_g	51391.6	0. 00
^4A_g	53111.9	46.83
^4B_u	56340.6	0. 00
^4A_g	56471.2	0. 00
^4B_g	56656.7	0.00
^4A_g	56659.9	35.73
^4B_u	56693.8	36.41
^4A_u	56696.2	0. 00
^4B_g	57227	0. 43
^4A_u	57326.2	0. 00
^4B_g	59004.6	0. 00
^4A_g	59092.5	11.72
^4AU	59258.6	

[a] For high-spin state (2S + 1 = 4), the full optimized structures have C_{2h} symmetry (a weakly distorted octahedron).

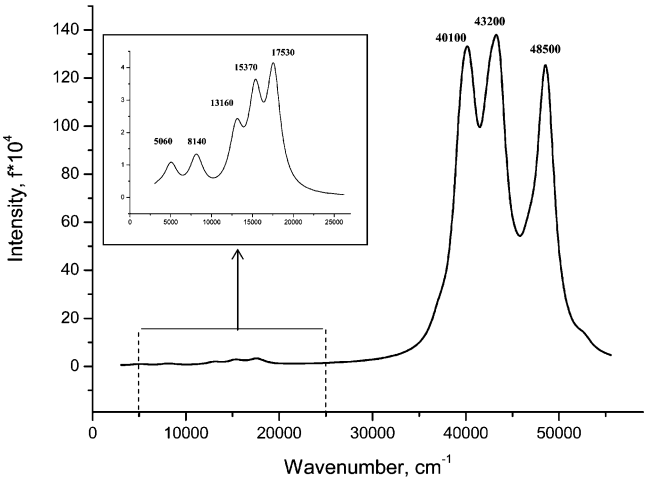

Figure 8. The calculated electronic spectrum for the high-spin state Co^{2+} complex modeling a rigid environment in the crystalline monoclinic $CoZr_4(PO_4)_6$ phase following ref 29.

4.2. Five-fold Coordinated Complexes. *High-Spin Complexes.* For the crystalline high-temperature phases of complex framework Co−Zr phosphates, the coordination environment of Co was modeled by a structure shown in Figure 4. Here, the geometry of the oxygen framework around the Co cation was fixed, while positions of the boundary atoms X were determined from the minimum of the full energy. The results of calculations are shown in Figure 8 and summarized in Table 4. Since the first coordination sphere of a Co^{2+} cation is comprised of only four oxygen atoms, while the fifth atom is situated at a bigger distance, for comparison, calculations have also been carried out for the model of the local environment without that oxygen atom (Table 4). As follows from these results, the addition of a fifth atom rather strongly affects spectra, especially in the UV range. In the vicinity of the absorption edge, both the number

TABLE 4: Excitation State Spectrum of High-Spin Co^{2+} Cations in a Model of the Rigid Environment[29] Corresponding to $[Co(d^7)(OX_2)_4]^{2+}$ and $[X_2O]-Co(d^7)(OX_2)_4]^{2+}$ Complexes

$Co[OX_2]_4$		$[X_2O]-Co[OX_2]_4$	
excitation energy, cm^{-1}	oscillator strength, $f \times 10^4$	excitation energy, cm^{-1}	oscillator strength, $f \times 10^4$
3147	0.17	3368	0.20
6539	0.59	5032	1.00
8136	1.32	8146	1.26
11835	1.78	13030	2.03
15452	4.73	15348	3.18
18095	5.03	17603	4.15
37500	96.42	37117	13.29
37647	48.63	39452	100.89
39624	46.58	39873	0.89
39848	5.87	40115	55.48
40275	23.33	40497	89.31
41471	80.63	41954	14.04
41910	13.49	42314	22.43
42712	42.85	42611	73.45
44131	36.02	43503	138.12
46320	41.60	43874	19.83
49475	262.32	45243	6.87
50592	14.38	45608	7.07
52241	28.11	46767	34.16
		48351	110.76
		48832	104.81
		52641	7.30

of transitions and their intensity change, while the position and intensity of the UV high-frequency part of the spectrum are not sensitive to the presence of a fifth atom. The model not taking into account the fifth atom apparently overestimates absorption at ~37500 cm^{-1}. However, in the d−d range, a distorted tetrahedron model better describes the spectrum of crystalline samples, since it predicts a band at ~11800 cm^{-1} visible as an increase of absorption between ~12500 and 10000 cm^{-1} (Figure 5). In contrast, a band at ~13000 cm^{-1} predicted by a model including the fifth atom is not observed. Comparison of the results presented in Tables 2 and 4 revealed that distortion of the tetrahedron and effect of the second coordination sphere decrease the oscillator strength in the d−d range, while increasing the bands splitting. However, all considered models based upon a rigid structure do not explain the appearance of bands in the 18500−22500 cm^{-1} range observed in the spectra of all crystalline samples. This discrepancy can arise due to the accepted model of the rigid framework. Moreover, single-crystal structural parameters of the coordination sphere of Ni cations in framework zirconium phosphates[29] used for these calculations are not necessarily adequate for the case of Co cations.

To deal with this problem, calculations have been carried out for the case of a soft framework when the oxygen environment around Co cations is fully relaxed. For the high-spin state of cobalt, this optimization results in several isomeric configurations. Figure 9 shows results of calculations for two of the most stable isomers such as the trigonal bipyramid (A) and the square pyramid (B). All electronic excitations are summarized in Table 5. For the high-frequency band position in the d−d transition range, calculations give values ~21000 cm^{-1} for the trigonal bipyramid and ~21200 cm^{-1} for the square pyramid. Hence, for those configurations, a blue shift of d−d transition bands occurs along with a noticeable decline of the oscillator strength as compared with distorted tetrahedral complexes. With due regard for this feature and possible distortion of the structure of these complexes by the zirconium phosphate framework, the band at ~12500−13000 cm^{-1} with a rather low oscillator strength predicted for the regular trigonal bipyramid could not

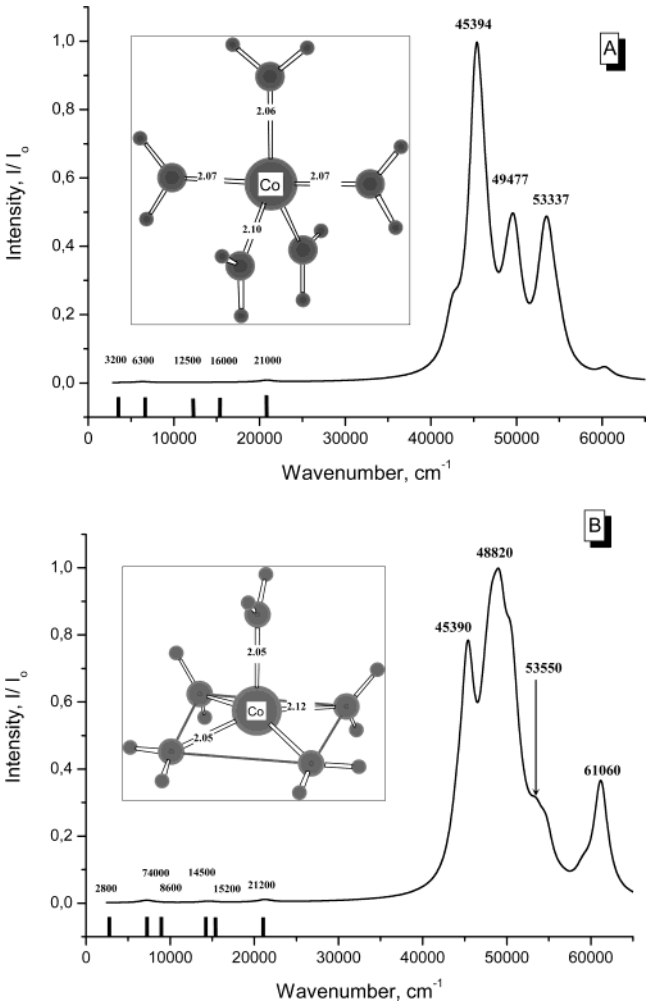

Figure 9. The calculated electronic spectra of high-spin states for the most stable $[Co(d^7)(OX_2)_5]^{2+}$ isomers: (A) trigonal bi-pyramid, (B) square pyramid.

be experimentally observed. Taking into account that in studied dispersed samples some amount of water is present in the lattice up to 900 C° as judged by the thermal analysis data,[20] and water molecules are certainly able to coordinate Co cations, a high-frequency component in the d−d region can be assigned to the configurations considered. As for the charge-transfer bands, their three-peak pattern rather close to the experimentally observed one is worth noting.

Calculations of the electronic spectra of 5-fold coordinated Co cations in the oxygen environment allows us also to understand the specificity of the spectral features of Co complexes with other ligands. Thus, a high-spin trigonal−bipyramidal complex $Co(Me_6tren)Cl^+$ with C_{3v} symmetry is characterized by absorption bands at <4000, 5800, 12600, 15500, and 20200 cm^{-1}.[60] Comparison of these features with the results presented in Figure 9A and Table 5 revealed that nonempirical calculations predict rather good spectra of those complexes in the visible range. Thus, calculated intensity is the highest for the band at ~21000 cm^{-1}, which agrees well with the known data.

The spectral features of high-spin square pyramidal complexes, both experimental and calculated, are not too different from those of the complexes with trigonal bipyramidal symmetry.[28] Thus, for the square pyramidal β-$Co(paphy)Cl_2$ complex, bands at ~4800, 7500, 12500 (weak), 1500 (shoulder), 16000, 17500, and 21000 cm^{-1} are observed.[28] Comparison with the calculated spectrum for a Co complex with C_{4v} symmetry

TABLE 5: Excitation-State Spectrum of Optimized Five-fold Coordinated Complex $[Co(d^7)(OX_2)_5]^{2+}$ [a]

square pyramid			trigonal bipyramid		
symmetry (group C_s)	energy, cm^{-1}	oscillator strength, $f \times 104$	symmetry (group)	energy, cm^{-1}	oscillator strength, $f \times 10^4$
A″	2683	0.29	A_2	3201	0. 00
A′	7238	2.02	B_1	6330	1.35
A″	8580	0.10	B_1	12460	0. 46
A′	14555	0.75	B_2	12809	0. 47
A″	15133	0.16	A_2	16131	0.00
A″	21258	2.16	A_1	20819	1.70
A′	44038	30.19	A_1	42525	51.83
A′	45350	171.85	B_2	45288	325.07
A″	47151	0.02	B_1	46195	74.88
A″	47404	60.75	B_2	46816	10.67
A″	48179	111.40	B_2	48943	44.70
A″	48974	29.12	A_1	49522	50.60
A′	49221	116.72	A_1	49852	78.93
A′	50536	133.24	A2	50200	0.00
A″	51444	19.32	A2	51019	0.00
A′	52092	6.46	B_2	52913	21.74
A′	52492	5.65	B_1	53272	2.46
A′	53451	33.09	A_1	53289	78.63
A′	53829	1.30	B_2	53392	0.03
A′	54666	35.86	A_1	53824	74.81
A″	56651	3.47	B_2	54909	32.74

[a] For high-spin state ($2S + 1 = 4$) the full optimized structures have C_s symmetry (weakly distorted square pyramid) and C_{2v}. one (distorted trigonal bipyramid).

(Table 3) demonstrates rather good agreement of the experimental and calculated spectra.

Low-Spin Complexes. Table 6 and Figure 10 show results of the spectra calculation for the low-spin square pyramidal and trigonal bipyramidal complexes of Co^{2+} cations. For the distorted square pyramid the position of the strongest bands in the d−d transition range at ∼17000, 18000, and ∼21000 cm^{-1} reasonably agree with those observed in samples calcined at temperatures up to 500 °C. Bands at ∼15000 cm^{-1} observed in these samples can thus be assigned to admixture of high-spin Co cations in the distorted tetrahedral environment (vide supra). The positions of the charge-transfer bands for low-spin square pyramidal complexes are also rather close to the experimentally observed ones. This implies that these complexes could be indeed formed in samples where low-spin cobalt(II) states dominate.

In contrast, spectral features of trigonal bipyramidal complexes of low-spin Co^{2+} cations drastically differ from those observed experimentally. Namely, very strong absorption in the range ∼25000−30000 cm^{-1} with the oscillator strength exceeding that of the charge-transfer bands (Figure 10 B) was not revealed for any studied sample. Moreover, very weak charge-transfer bands at ∼50000 cm^{-1} predicted for this complex are also in disagreement with the experimental data. This suggests that complexes of such a type are not formed in the complex Co−Zr framework phosphates. However, these results in general agree with the statement of Lever[28] that for low-spin 5-fold coordinated complexes of Co^{2+} anomalous high absorption in the d−d range is observed. Thus, for low-spin trigonal bipyramidal complexes with cobalt cations in a strong crystalline field,[61,62] along with intense transition at ∼20000 cm^{-1}, (extinction coefficient ∼ 600 L/(mol cm), a band at ∼25000 cm^{-1} with a comparable intensity is observed. As follows from comparison with Figure 10 B, our results correctly reproduce those specific features of the electronic spectra of Co^{2+} low-spin trigonal bipyramidal complexes.

TABLE 6: Excitation-State Spectrum of Optimized Five-fold Coordinated Complex $[Co(OX_2)_5]^{2+}$ [a]

square pyramid			trigonal bipyramid		
symmetry	energy, cm^{-1}	oscillator strength, f × 10^4	symmetry	energy, cm^{--1}	oscillator strength, f × 10^4
A″	8467	0.63	B1	14961.68	3.38
A′	9094	0.75	A1	18746.55	16.87
A″	10131	0.00	B2	19221.72	126.31
A″	13330	0.07	B2	21909.91	56.86
A′	17064	4.24	B1	25146.97	126.66
A″	17726	3.67	B2	25454.90	100.32
A′	21484	0.27	A1	25630.08	54.59
A′	38044	2.58	A1	27252.01	21.25
A′	43671	69.43	B2	28701.66	483.25
A′	44744	0.97	B1	32513.29	324.72
A′	45080	11.17	A1	37128.14	168.04
A″	45817	1.77	A1	39695.99	99.67
A″	47169	0.01	B2	40039.90	32.91
A″	49961	16.76	B1	42345.844	2.49
A″	50273	15.24	A1	42868.061	26.44
A′	51172	82.47	B2	46972.361	3.77
A′	51547	16.76	A1	47350.544	10.03
A′	52218	43.23	B2	48325.520	8.37
A″	52548	37.17	B1	49142.871	0.54
A″	53042	31.98	B2	53644.242	40.32
A′	54053	25.55	A1	56849.614	134.81
A"	54874	2.29	B1	57887.425	30.08
			B1	58265.874	47.08
			B2	59033.853	166.93
			B1	60006.054	97.18
			A1	60042.686	16.05
			A	61805.656	209.82

[a] For low-spin state ($2S + 1 = 2$) the full optimized structures have C_s symmetry (weakly distorted square pyramid) and C_{2v} one (weakly distorted trigonal bipyramid).

5. Discussion

All spectral features for a given sample could not be assigned to only one type of Co complexes. Instead, a combination of several states is required to describe the experimental spectra. For the low-temperature (<500 °C) samples, the situation is even more complex due to the presence of cobalt cations in high-spin and low-spin states. At least it is clear that Co cations in a relatively symmetric octahedral environment (such as in hexa-aquo complexes or in positions occupied by Zr cations in framework zirconium phosphates) could not be present in any substantial (exceeding uncertainty of analysis ∼10−20%) amount in samples considered here. Hence, the degree of positional disordering between Co and Zr cations appears to be small (if present at all) even in the X-ray amorphous samples. Instead, main features of the experimental spectrum for the crystalline sample calcined at 500 °C (Figure 5) are relatively well reproduced in Figure 11 by superposition of the theoretical spectra for slightly distorted tetrahedral high-spin complex (20% contribution) and low-spin square pyramid (80% contribution). Though this comparison is of a purely qualitative nature due to the absence of independent data on the real composition and geometries of Co complexes and their relative amounts as well as due to apparent disregard for the chemical specificity of phosphate groups as ligands, nevertheless, in the first approximation, it appears to be quite satisfactory. Certainly, for the sample considered, the presence of high-spin cobalt cations in another coordination environment such as distorted trigonal bipyramid and square pyramid could not be excluded as well.

Calculated excitation spectra for high-spin and low-spin complexes taken together with the magnetic susceptibility data allow us also to explain the experimentally observed variation

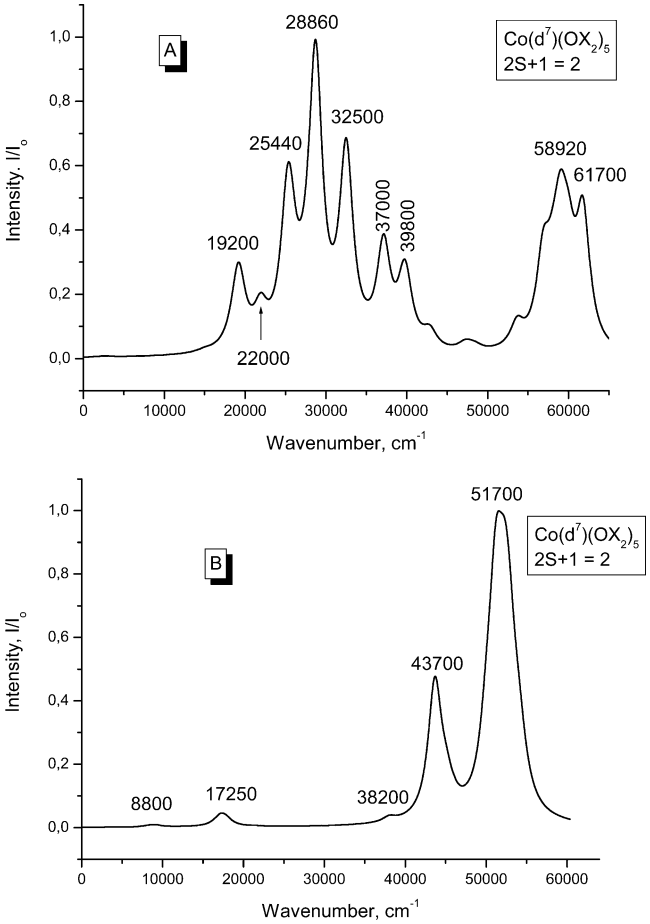

Figure 10. The calculated electronic spectra of low-spin states for two stable $[Co(d_7)(OX_2)_5]^{2+}$ isomers: (A) trigonal bipyramid, (B) square pyramid.

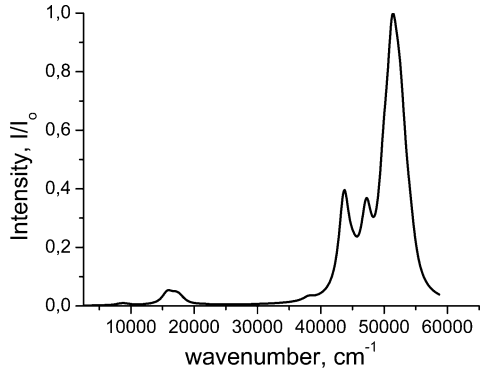

Figure 11. Modeling of the experimental spectrum for a crystalline $CoZr_4(PO_4)_6$ sample calcined at 500 °C by superposition of spectra for optimized high-spin tetrahedral and low-spin square pyramidal complexes in a 2:8 ratio.

of the UV bands intensity and position with the temperature of calcinations (Figure 5). Thus, for high-spin Co^{2+} cations in weakly distorted tetrahedral (Table 2), square pyramidal, and trigonal bipyramidal (Table 5) coordination present in the dried sol sample with an amount up to 50%, the most intense transitions in the 45000−50000 cm^{-1} range are characterized by the oscillator strength ∼100−300 units. For the sample calcined at 500 °C, where the amount of cations in the high-spin state is much lower, a low-spin state with a square pyramidal coordination appears to dominate. For the latter complexes, the oscillator strength in the considered UV range is 2−3 times lower (Table 6), which certainly correlates with the experimentally observed decline of absorption. On the other hand, in the crystalline sample annealed at 700 °C, all cations are in the high-spin state, which explains the increase of the UV absorption for this sample. Moreover, for distorted tetrahedral coordination in the frames of the rigid model (vide supra) both with and without the fifth atom being taken into account, the strongest transitions are shifted to 50000 cm^{-1}, which seem to correlate with the high-frequency shift of the UV absorption for the crystalline sample as compared with the amorphous sample.

TABLE 7: Dependence of Bond Lengths Co−O, Co Charge, Co Spin Density, and Energy Difference ΔE of Optimized Clusters $[Co(d^7)(OX_2)_n]^{2+}$ on Coordination Number (n) in Different Spin States. $\Delta E = E$(low spin) − E(high spin)

coordination, n	4	5	5	5
		Low Spin: $2S + 1 = 2$		
geometry	square	square pyramid	experimental,[31] Fig. 4	bipyramid
bond length, Å	1.94−1.96	1.96−2.16	1.89−2.26, 2.83	2.05−2.19
charge (Co)	1.04	0.93	1.02	0.96
spin density (Co)	1.04	0.99	1.01	0.99
		High Spin: $2S + 1 = 4$		
geometry	tetrahedral	square pyramid	experimental,[31] Fig. 4	bipyramid
bond length, Å	2.01	2.05−2.12	1.89−2.26, 2.83	2.06−2.10
charge	1.10	1.00	1.06	1.02
spin density	2.85	2.83	2.85	2.82
ΔE, kcal/mol	24	24	27	87

The results of theoretical simulation imply that in dispersed complex framework zirconium phosphates the ground state of Co^{2+} cations is the high-spin state ($2S + 1 = 4$). The energy of the low-spin state ($2S + 1 = 2$) is higher for ∼30000 cm^{-1} for 5-fold coordination and for ∼10000 cm^{-1} (25−30 kcal/mol) for 4-fold coordination (Table 7). Thus, for a low coordination, the energy difference substantially decreases. The appearance of a low-spin state is related to the rearrangement of the electron distribution on the d-orbitals without any substantial transfer of the electron density to neighboring atoms. Indeed, according to calculations, the Co−O bond lengths for low-spin and high-spin states are approximately the same (Table 7), while any substantial cation−anion charge transfer is expected to cause bond length variation. Comparison of the Co−O bond lengths for $CoZr_4(PO_4)_6$ and $Co_3[BPO_7]$[48] shows that they are also close to each other. Therefore, low-spin states of cobalt cations revealed for Co−Zr framework phosphates appear to be caused by the same factors as in the case of $Co_3[BPO_7]$.[48] The magnetic measurements and theoretical calculations suggest that these low-spin states are metastable states corresponding to a local minimum of the potential energy. Hence, while the temperature of sample calcination increases, they should transform into the high-spin states, which is indeed observed for complex framework Co−Zr phosphates.

The results obtained in this work allow the conclusion that in complex crystalline framework zirconium phosphates with a monoclinic structure synthesized via a sol−gel route, cations of Co are mainly situated in bulky irregularly shaped polyhedra. Rearrangement of the flexible framework ensures a local coordination of Co cations by up to four oxygen anions in the first coordination sphere with the fifth anion being located in the second coordination sphere. These results agree with the model suggested by Joanneaux et al. for the local environment of Ni cations in that system.[29] Here, oxygen atoms of the Ni first coordination sphere are shared both with the Zr octahedron and four different phosphate groups. However, a rigid model of this type does not allow us to satisfactorily describe all spectral features for powdered crystalline samples of $CoZr_4$-

$(PO_4)_6$ in the visible range, which is the most sensitive to the local symmetry of the oxygen environment. This can be explained by a higher flexibility of the structure of small particles, their disordering, as well as by the effect of residual water retained in the lattice of dispersed framework phosphates up to 900 °C.[20] As a result, Co cations can acquire 5-fold coordination of the trigonal bipyramidal or square pyramidal types, where phosphate groups participate as monodentate ligands. For amorphous or partially crystalline samples, due to disordering in stacking of the lantern-type fragment (vide supra), or retaining of fragments with the structure of layered zirconium phosphates, the possibility of Co cations polydentate coordination by phosphate groups could exist. This appears to favor stabilization of the low-spin state of Co^{2+} cations, which certainly require further studies. This specific feature makes poorly crystallized cobalt-containing framework zirconium phosphates principally different from other known Co-containing systems such as silicates, zeolites, etc.

From the methodological point of view, present results are certainly in favor of models suggested by Klier[58] and Sobalik et al.[32] for dehydrated Co-containing zeolites, in which appearance of bands in the visible range at ~20000−22000 cm^{-1} is assigned to the effects of the second coordination sphere while the chemical bonds are formed between a Co cation and four (or three) oxygen atoms of the first coordination sphere. As a result, traditional assignment of bands in this range to octahedrally coordinated Co cations[32,58,63] by a simple analogy with the bulk oxide systems[47] should be considered with caution if estimation of the extinction coefficients is absent.

For complex Co-containing phosphate systems, tetrahedral (or similar low) coordination of Co cations seems to be a rather general feature. Apart from CoAPO (vide supra), for the orthorhombic $Na_2CoP_2O_7$ phase,[64,65] axially distorted tetrahedral coordination of Co cations (point group D_{2d}) with similar parameters of the electronic spectra (bands in the visible range at ~ 16000, 17500, 19600, and 21000 cm^{-1}) was revealed. Identical spectral features in the visible range were observed for the monoclinic $Li_{2-x}Co_xBaP_2O_7$ phase, though they were assigned to Co cations both in the tetrahedral positions (instead of Li cations) and vacant octahedral positions.[66] For this system, the intensity of bands attributed to Co cations in different environments was comparable. Taking into account the results of the present work, assignment of the bands observed in the d−d range to Co cations located in strongly distorted tetrahedral positions vacant in the parent $Li_2BaP_2O_7$ phase appears to be more plausible.

In the cobalt phosphate of $Co_3(PO_4)_2$ composition with the olivine structure, along with the rather symmetric octahedral positions, a strongly distorted trigonal bipyramidal environment similar to that considered in the present work but with even stronger variation of the bond length and angles is realized.[67,68] In the spectra of this compound, bands at 4760, 9260, and 17200 cm^{-1} were assigned to Co cations in the octahedral coordination, while bands at 5900, 11000, and 20400 cm^{-1}were assigned to the Co cations in a trigonal environment.[69] For this compound, the intensities of bands assigned to different polyhedra were also comparable. Taking into account that molar extinction coefficients even for distorted octahedra are low (vide supra), the results obtained in our work allow us to assume that all bands observed for this compound can be due to Co cations in a strongly distorted trigonal environment. Indeed, according to Lever,[28] for high-spin trigonal bipyramidal complexes molar extinction coefficients are in the range of 50−500 L/(mol cm), while for the octahedral complexes distorted up to C_2 symmetry, molar extinction coefficients are less than 10 L/(mol cm). Since in the structure of Co phosphates the ratio of the octahedral to trigonal positions is equal to 1 or 2 (as dependent upon the phase structure), one can conclude that bands corresponding to Co cations in octahedral positions will not be observed at all.

By analogy with zeolites, a relatively low coordination of transition metal cations, especially those situated at the surface of framework phosphate systems, appears to be of a great importance for the efficient activation of hydrocarbons, in particular, for the processes of alkanes oxidative dehydrogenation into alkenes at short contact times.[5]

6. Conclusions

The first-principle TDDFT method has been successfully applied for modeling of the full electronic spectrum of cobalt cations in the matrix of framework zirconium phosphates and their precursors—amorphous sols. Comparison of the theoretical results with the known data for Co complexes and CoAPO demonstrated that the suggested approach allows us to adequately describe and predict the spectral features of at least Co-containing compounds. Analysis of acquired and published earlier data implies that both for complex and simple Co-containing bulk phosphates the Vis spectra corresponds to Co cations in distorted low-coordinated polyhedra such as tetrahedron, trigonal bipyramid, etc.

Acknowledgment. This study was supported by the Russian Foundation for Basic Research under Grant N 02-3-33351a and Grant SS-1140.2003.3 for Scientific School support, G.M.Z. is also grateful to CRDF (project REC-008). The authors are deeply grateful to N. M. Bazhin, V. F. Anufrienko, and E. A. Paukshtis for very helpful discussions of results and to N. A. Paukshtis, T. Larina, and S. V. Koshcheev for spectra recording and their treatment.

References and Notes

(1) Kung, H. H.; Kung, M. C. *Catal. Today* **1996**, *30* (1−3), 5.
(2) Li, Y.; Armor, J. N. *Appl. Catal. B: Environ.* **1993**, *2*, 239.
(3) Li, Y.; Armor, J. N. *J. Chem. Soc., Chem. Commun.* **1997**, *20*, 2013.
(4) Sadykov, V. A.; Pavlova, S. N.; Frolova, Yu. V.; et al. *4th World Congress on Oxidative Catalysis*, Berlin, 2001.
(5) Pavlova, S. N.; Sadykov, V. A.; Frolova, Yu. V.; Saputina, N. F.; Vedenikin, P. M.; Zolotarskii, I. A.; Kuzmin, V. A. *Chem. Eng. J.* **2003**, *91*, 227.
(6) Alamo, J. *Solid State Ionics* **1993**, *63−65*, 547.
(7) Sigarev, S. E. *Kristallografiya* **1992**, *37* (1), 1055.
(8) Alamo, J.; Roy, R. *J. Mater. Sci.* **1986**, *21*, 444.
(9) Pet'kov, V. I.; Dorohina, G. I.; Orlova, A. I. *Kristallografiya* **2001**, *46*, 76.
(10) Goodenough, J. B.; Hong, H. J.; Kafalas, J. A. *Mater. Res. Bull.* **1976**, *11*, 173.
(11) Roy, R.; Vance, E. R.; Alamo, J. *Mater. Res. Bull.* **1982**, *17*, 585.
(12) Alamo, J.; Roy, R. *J. Am. Ceram. Soc.* **1984**, *63*, C.78.
(13) Clearfield, A.; Thakur, D. S. *Appl. Catal.* **1986**, *26*, 1.
(14) Segawa, K.; Kurusu, Y.; Nakajima, Y.; Kinishita, M. *J. Catal.* **1985**, *94*, 491.
(15) Frinaeza, T. N.; Clearfield, A. *J. Catal.* **1984**, *85*, 398.
(16) Ai, M. *Catal. Today* **1999**, *52*, 65.
(17) Sadykov, V. A.; Pavlova, S. P.; Chaikina, M. V.; Zabolotnaya, G. V.; Maksimovskaya, R. I.; Tsybulya, S. V.; Burgina, E. B.; Zaikovskii, V. I.; Litvak, G. S.; Frolova, Yu. V.; Kochubei, D. I.; Kriventsov, V. V.; Paukshtis, E. A.; Kolomiichuk, V. N.; Ivanov, V. P.; Anufrienko, V. F.; Boldyreva, N. N.; Kuznetsova, N. N.; Lunin, V. V.; Agrawal, D.; Roy, R. *Chemistry in Sustainable Development* **2002**, *10*, 227.
(18) Chaikina, M. V.; Sadykov, V. A.; Pavlova, S. N.; Zabolotnaya, G. N.; Maximovskaya, R. I.; Kriventsov, V. V.; Kochubey, D. I.; Burgina, E. B.; Roy, R.; Agrawal, D. K. *J. Mater. Synth. Process.* **2000**, *8* (5/6), 279.
(19) Sadykov, V. A.; Pavlova, S. P.; Zabolotnaya, G. V.; Chaikina, M. V.; Maksimovskaya, R. I.; Tsybulya, S. V.; Burgina, E. B.; Zaikovskii, V. I.; Litvak, G. S.; Frolova, Yu. V.; Kochubei, D. I.; Kriventsov, V. V.;

Paukshtis, E. A.; Kolomiichuk, V. N.; Kuznetsova, N. N.; Lunin, V. V. *Kinet. Katal.* **2001**, *42* (3), 432.
(20) Pavlova, S. N.; Sadykov, V. A.; Zabolotnaya, G. V.; Maximovskaya, R. I.; Zaikovskii, V. I.; Tsybulya, S. V.; Burgina, E. B.; Chaikina, M. V.; Agrawal, D.; Roy, R. *Solid State Ionics* **2001**, *141*−*142*, 683.
(21) Kriventsov, V. V.; Kochubey, D. I.; Sadykov, V. A.; Pavlova, S. N.; Zabolotnaya, G. V. *Nucl. Instr. Methods Phys. Res. A* **2001**, *470*, 1.
(22) Sadykov, V. A.; Pavlova, S. N.; Zabolotnaya, G. V.; Maximovskaya, R. I.; Kochubey, D. I.; Kriventsov, V. V.; Odegova, G. V.; Ostrovskii, N. M.; Tsybulya, S. V.; Burgina, E. B.; Zaikovskii, V. I.; Chaikina, M. V.; Lunin, V. V.; Roy, R.; Agrawal, D. *Mater. Res. Innov.* **2000**, *3*, 276.
(23) Morgan, D.; Ceder, G.; Saidi, M. Y.; Barker, J.; Swoyer, J.; Huang, H.; Adamson, G. *Chem. Mater.* **2002**, *14*, 4684.
(24) Sigarev, S. E. *Kristallografiya* **1992**, *37* (4), 1055.
(25) Frolova, Yu. V.; Sadykov, V. A.; Pavlova, S. N.; Burgina, E. B.; Tsybulya, S. V.; et al. In preparation.
(26) Jacono, R. L.; Cimino, A.; Schuit, G. C. A. *Gaz. Chim. Ital.* **1973**, *103*, 1281.
(27) Asmolov, G. N.; Krylov, O. V. *Kinet. Catal.* **1971**, *12*, 453.
(28) Lever, A. P. B. *Inorganic Electronic Spectroscopy*; Elsevier: New York, 1968, 1984; p 319.
(29) Jouanneaux, A.; Verbaere, A.; Piffard, Y. *Eur. J. Solid State Inorg. Chem.* **1991**, *28*, 683.
(30) Collin, G.; Comes, R.; Boilot, J. P.; Colomban, Ph. *J. Phys. Chem. Solids* **1986**, *47*, 843.
(31) Pet'kov, V. I.; Orlova, A. I.; et al. *Kristallografiya* **2000**, *45* (1), 36.
(32) Sobalík, Z.; Dědeček, J.; Kaucky, D.; Wichterlová, B.; Drozdová, L.; Prins, R. *J. Catal.* **2000**, *194*, 330.
(33) Kurazhkovskaya, V. S.; Orlova, A. I.; Pet'kov, V. I.; Kemenov, D. V.; Kaplunnik, L. N. *Zh. Struct. Khim.* **2000**, *41*, 74.
(34) Parr, R. G.; Yang, W. *Density-Functional Theory of Atoms and Molecules*; Oxford University Press: New York, 1989.
(35) Runge, E.; Gross, E. K. U. *Phys. Rev. Lett.* **1984**, *52*, 997.
(36) Van Gisbergen, S. J. A.; Snijders, J. G.; Baerends, E. J. *J. Chem. Phys.* **1995**, *103*, 9347.
(37) Görling, A.; Heinze, H. H.; Ruzankin, S. Ph.; Staufer, M.; Rösch, N. *J. Chem. Phys.* **1999**, *110*, 2785.
(38) Adamo, C.; Scuseria, E.; Barone, V. *J. Chem. Phys.* **1999**, *111*, 2889.
(39) Hirata, S.; Lee, T. J.; Head-Gordon, M. *J. Chem. Phys.* **1999**, *111*, 8904.
(40) Broclawik, E.; Borowski, T. *Chem. Phys. Lett.* **2001**, *339*, 433.
(41) Ricciardi, G.; Rosa, A.; Baerends, E. J.; van Gisbergen, S. A. J. *J. Am. Chem. Soc.* **2002**, *124*, 12319.
(42) Cavillot, V.; Champagne, B. *Chem. Phys. Lett.* **2002**, *354*, 449.
(43) Bazhin, N. M. *Izvestiya SO AN SSSR, Ser. Khim.* **1987**, *2*, 29.
(44) Aoki, M. *Introduction to Optimization Techniques*, Moskow, 1977; p 144.
(45) Gmelin, *Handbuch der Anorg. Chem, 8 Aufl, Kobalt, N. 58, Teil B, Verlag Chemie*, G. M. B. H., Berlin, 1932.
(46) Khassin, A. A.; Anufrienko V. F.; Ikorskii, V. N.; Plyasova, L. M.; Kustova, G. N.; Larina, T. V.; Molina, I. Yu.; Parmon, V. N. *Phys. Chem. Chem. Phys.* **2002**, *4*, 4236.
(47) Khalil, M. I.; Logan, N.; Harris, A. D. *J. Chem. Soc., Dalton Trans.* **1980**, 314.
(48) Yilmaz, A.; Bu, X.; Kizilyalli, M.; Kniep, R.; Stucky, G. D. *J. Solid State Chem.* **2001**, *156*, 281.
(49) Aatiq, A.; Ménétrier, M.; Croguennec, L.; Suard, E.; Delmas, C. *J. Mater. Chem.* **2002**, *12*, 2917.
(50) Bykov, A. B.; Chirkin, A. P.; Demyanets, L. N.; Doronin, S. N.; Genkina, E. A.; Ivanov-Shits, A. K.; Kondratyuk, I. P.; Maksimov, B. A.; Mel'nikov, O. K. *Solid State Ionics* **1990**, *38*, 31.
(51) Becke, A. D. *Phys. Rev.* **1986**, *A33*, 2786.
(52) Becke, A. D. *J. Chem. Phys.* **1993**, *98*, 5648.
(53) Lee, C.; Yang, W.; Parr, R. G. *Phys. Rev.* **1988**, *B37*, 785.
(54) Stevens, W.; Bash, H.; Krauss, J. *J. Chem. Phys.* **1984**, *81*, 6026.
(55) Cundari, T. R.; Stevens, W. J. *J. Chem. Phys.* **1993**, *98*, 5555.
(56) Frisch, M. J.; Trucks, G. W.; Schlegel, H. B.; et al. *Gaussian Revision A.11*; Gaussian Inc.: Pittsburgh, PA, 2001.
(57) Šponer, J.; Čejka, J.; Dědeček, J.; Wichterlova, B. *Microporous Mesoporous Mater.* **2000**, *37*, 117.
(58) Verbeckmoes, A. A.; Uytterhoeven, M. G.; Schoonheydt, R. A. *Zeolites* **1997**, *19*, 180.
(59) Klier, K.; Kellerman, R.; Huta, P. J. *J. Phys. Chem.* **1974**, *61*, 4224.
(60) Ciampolini, M.; Nardi, N. *Inorg. Chem.* **1972**, *11*, 1466.
(61) Norget, M. J.; Thornley, J. H. M.; Venanzi, L. M. *J. Chem. Soc. (A)* **1967**, 540.
(62) Norget, M. J.; Thornley, J. H. M.; Venanzi, L. M. *Inorg. Chim. Acta* **1968**, *2*, 107.
(63) Hartmann, M.; Kevan, L. *Chem. Rev.* **1999**, *99* (3), 635.
(64) Derouet, J.; Beaury, L.; Porcher, P.; Sanz, F.; Ruiz, C.; Parada, C.; Saez-Puche, R. In *Books of Abstracts, VIIth Europ. Conf. Solid State Chem., Sept. 15*−*18, Madrid, Spain* **1999**, *2*, 273.
(65) Porcher, P.; Couto dos Santos, M. A.; Malta, O. M. L. *Phys. Chem. Chem. Phys.* **1999**, *1*, 397.
(66) Kovacheva, D.; Nikolov, V.; Petrov, K.; Rojas, R. M.; Herrero, P.; Rojo, J. M. *J. Mater. Chem.* **2001**, *11*, 444.
(67) Nord, A. G. *Mater. Res. Bull.* **1977**, *12*, 563.
(68) Nord, A. G.; Stefanidis, T. *Z. Kristallogr.* **1980**, *153*, 141.
(69) Aaddane, A.; Kacimi, M.; Ziyad, M. *Catal. Lett.* **2001**, *73*, 47.